

Kondo effect in a hybrid superconductor–quantum-dot–superconductor junction with proximity-induced p -wave pairing states

Lin Li,^{1,*} Jin-Hua Sun,² Wei Su,¹ Zhen-Hua Wang,³ Dong-Hui Xu⁴,⁵ Hong-Gang Luo,^{5,6} and Wei-Qiang Chen^{7,8,†}

¹*Department of Physics and Electronic Engineering, and Center for Computational Sciences, Sichuan Normal University, Chengdu 610068, China*

²*Department of Physics, Ningbo University, Ningbo 315211, China*

³*Shenzhen Key Laboratory of Advanced Thin Films and Applications, College of Physics and Optoelectronic Engineering, Shenzhen University, Shenzhen 518060, China*

⁴*Department of Physics, Hubei University, Wuhan 430062, China*

⁵*School of Physical Science and Technology and Key Laboratory for Magnetism and Magnetic Materials of the Ministry of Education, Lanzhou University, Lanzhou 730000, China*

⁶*Beijing Computational Science Research Center, Beijing 100084, China*

⁷*Institute for Quantum Science and Engineering and Department of Physics, Southern University of Science and Technology, Shenzhen 518055, China*

⁸*Shenzhen Key Laboratory of for Advanced Quantum Functional Materials and Devices, Southern University of Science and Technology, Shenzhen 518055, China*

 (Received 21 January 2021; revised 14 March 2021; accepted 15 March 2021; published 22 March 2021)

We study the transport of a hybrid superconductor–quantum-dot–superconductor junction, dominated by the interplay between the Kondo effect and the proximity-induced p -wave pairing states. Each superconductor lead is fabricated with a semiconductor with Rashba spin-orbit coupling (RSOC) and the combination of an s -wave superconductor and a ferromagnet. The RSOC breaks the $SU(2)$ spin-rotation symmetry and creates the spin-triplet pairing components under the proximity-induced superconducting pairing interaction. Different from the s -wave pairing case, the Kondo screening of the dot spin involves the orbital angular momentum conserved transitions between the p -wave pairing states. The Zeeman field inherent from the ferromagnet removes the spin degeneracy of the quasiparticles excited in the triplet states. As a result, the spin-induced Yu-Shiba-Rusinov (YSR) state exhibits Zeeman-dependent splitting behaviors, and the splitting of the YSR state leads to the 0 - π phase transition when the ground state is a Kondo singlet. The temperature-dependent magnetic susceptibility indicates that the dot spin should be partially screened due to the breaking of time-reversal symmetry.

DOI: [10.1103/PhysRevB.103.125144](https://doi.org/10.1103/PhysRevB.103.125144)

I. INTRODUCTION

The Kondo effect, originating from the screening of the magnetic moment by conduction electrons, is one of the well-understood many-body phenomena in condensed-matter physics [1–3]. In recent decades, the Kondo effect in a quantum dot (QD), manifested as a zero-bias resonance peak, has been intensively investigated due to the high controllability [4,5]. In a QD coupled with an s -wave superconductor, the Kondo resonance is significantly suppressed due to the superconducting energy gap [6,7], and the low-energy transport is mainly determined by the behaviors of the spin-induced Yu-Shiba-Rusinov (YSR) state [8–11]. The competition between the Kondo effect and the superconducting pairing interaction in a hybrid superconductor-QD device generates two different ground states, namely, the magnetic doublet ($T_K < \Delta$) and the Kondo singlet state ($T_K > \Delta$) [12–20], where T_K is the normal-state Kondo temperature and Δ is the energy gap. The

quantum phase transition (QPT) between these two ground states takes place at $T_K/\Delta \sim 1$, which is indicated by the level-crossing behavior of the YSR state [18–21]. In the presence of Rashba spin-orbit coupling (RSOC), however, the phase boundary of the ground states depends on the strength of the RSOC rather than $T_K/\Delta \sim 1$ [22].

In unconventional superconductors, the orbital degrees of freedom play an important role in the Kondo effect [23–30]. In the spin-triplet $p_x + ip_y$ pairing state with a full energy gap, the local moment is partially quenched by the Kondo screening [29] and the ground state is always a spin doublet [27]. This result is quite different from the case of single magnetic impurity doped s -wave superconductors. In order to detect the fascinating physics induced by the magnetic moment in spin-triplet pairing states, we consider a Josephson junction composed of a QD coupled with two superconducting leads (S-QD-S) fabricated by the two-dimensional electron gas (2DEG) in a semiconductor with RSOC in proximity to a Bardeen-Cooper-Schrieffer (BCS) superconductor and a ferromagnetic insulator, as shown in the schematic diagram in Fig. 1(a). The spin-triplet pairing states, described by the order parameter $\Delta_T(\mathbf{k}) = i\sigma_y\Delta_0[\mathbf{d}(\mathbf{k}) \cdot \boldsymbol{\sigma}]$, would be created

*linli09@lzu.edu.cn

†chenwq@sustech.edu.cn

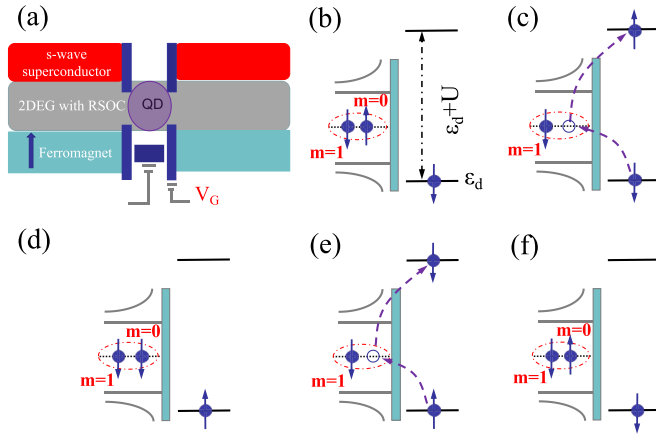


FIG. 1. (a) The schematic diagram of the Josephson junction made of a quantum dot (QD) and the superconducting leads fabricated by semiconductors with RSOC and the combination of an s -wave superconductor and a ferromagnetic insulator. The RSOC breaks the spin-rotation symmetry and creates spin-triplet p -wave pairing states. The local spin is directly coupled to only the $m = 0$ electron under the short-range scattering approximation. (b)–(d) The spin-down electron on the dot level is replaced by the spin-up electron with $m = 0$ in the triplet state through the virtual states. An equal spin pairing (ESP) state forms when the hole is filled by the spin-down electron tunneling out of the dot. (e) The spin-up electron on the dot level can be replaced by the spin-down electron with $m = 0$ in the ESP state. Correspondingly, the hole is filled by the spin-up electron hopping out of the dot, as shown in (f). The Kondo screening of the dot spin can be realized by the coherent superposition of these spin-flipping cotunneling processes, and the quasiparticles with $m = \pm 1$ form a spin-doublet state.

in the 2DEG with the aid of the RSOC and the superconducting pairing interaction [31,32], and the d -vector $\mathbf{d}(\mathbf{k}) = (-k_x, k_y, 0)$ with the time-reversal symmetry [33–35]. The Zeeman splitting inherited from the ferromagnetic insulator profoundly changes the superconducting pairing states, and even generates a spinless p -wave state in the topologically nontrivial phase [36,37]. Here, the hybrid junction described in Fig. 1(a) provides a controllable platform to study the transport dominated by the competition between the Kondo effect and these unconventional pairing states.

Different from the spin-singlet s -wave pairing states, the triplet p -wave states are composed of two electrons with orbital angular momentum $m = 0$ and $m = \pm 1$, respectively. The spectra of YSR states induced by a magnetic impurity in s -wave and p -wave pairing states exhibit qualitatively different behaviors [38]. In the present work, RSOC breaks the spin-rotation symmetry and results in the mixture of s -wave and p -wave pairing states in the leads. In Figs. 1(b)–1(f), we show the Kondo screening of the local moment by p -wave pairing states. Here, we consider the short-range scattering (s wave), namely, the local spin exchanges with only the $m = 0$ electrons. A spin-down electron on the dot level is replaced by the spin-up electron with $m = 0$ in the triplet state ($S_z = 0$) through the double or empty occupied virtual states, as shown in Figs. 1(b) and 1(c). The spin-down electron tunnels into the 2DEG and fills the hole in the lead, and an equal spin pairing (ESP) state with $S_z = -1$ forms in

Fig. 1(d). The spin-up electron on the dot level can be replaced by the spin-down electron with $m = 0$ exiting in the ESP state; then the spin-triplet state with $S_z = 0$ is restored by filling the hole in the lead [see Figs. 1(e) and 1(f)]. The Kondo screening of the dot spin can be realized by the coherent superposition of these tunneling processes. Similarly, the local moment can also be screened by the triplet states with $S_z = 0$ and $S_z = 1$. The most remarkable feature is that only the conduction electrons with $m = 0$ take part in the Kondo screening, while the quasiparticles with $m = \pm 1$ form a spin-doublet state [27–29]. In addition, the Kondo screening involves the transitions between different triplet pairs with the same total orbital angular momentum. The Zeeman field V_z removes the spin degeneracy of the quasiparticle in spin-triplet states. Thus, the YSR state exhibits Zeeman-dependent splitting behaviors, and the local moment is partially screened in this case. The splitting of the YSR state leads to a 0 - π phase transition or the suppression of the Josephson current, depending on the ground state of the system.

The paper is organized as follows. In Sec. II, we present the model of the Josephson junction fabricated by a QD coupled to the superconducting leads with the mixture of s - and p -wave pairing states, and set out the theoretical treatments. In Sec. III, we discuss the transport dominated by the interplay between the Kondo effect and the spin-triplet pairing states in the 2DEG. A brief summary is devoted to Sec. IV.

II. MODEL AND FORMALISM

The Hamiltonian of the hybrid S-QD-S junction reads

$$H = \sum_{\alpha} H_{\alpha} + H_{QD} + H_V, \quad (1)$$

where $H_{\alpha} = H_{\alpha 0} + H_{\alpha s} + H_{\alpha z}$ describes the leads ($\alpha = L, R$) with the mixture of s -wave and p -wave pairing states. The 2DEG with RSOC in the semiconductor can be described by the Hamiltonian

$$H_{\alpha 0} = \sum_{\mathbf{k}\sigma} \varepsilon_{\alpha\mathbf{k}} c_{\alpha\mathbf{k}\sigma}^{\dagger} c_{\alpha\mathbf{k}\sigma} + \sum_{\mathbf{k}} \lambda_{\alpha} \mathbf{k} (e^{-i\theta_{\mathbf{k}}} c_{\alpha\mathbf{k}\downarrow}^{\dagger} c_{\alpha\mathbf{k}\uparrow} + \text{H.c.}), \quad (2)$$

where $\varepsilon_{\alpha\mathbf{k}} = \frac{\mathbf{k}^2}{2m} - \mu_{\alpha}$ is the single-particle energy of conduction electrons and μ_{α} is the chemical potential. The operator $c_{\alpha\mathbf{k}\sigma}^{\dagger}$ ($c_{\alpha\mathbf{k}\sigma}$) denotes the creation (annihilation) of an electron with the momentum $\mathbf{k} (=k_x \hat{\mathbf{x}} + k_y \hat{\mathbf{y}})$ and the spin $\sigma (= \uparrow, \downarrow)$. λ_{α} is the strength of the RSOC to orient the spin of the electrons perpendicular to their momentum in the 2D plane, and $\theta_{\mathbf{k}} = \text{atan}(k_x/k_y)$ is the polar component of \mathbf{k} with $k = |\mathbf{k}|$. The proximity-induced superconducting pairing interaction in the 2DEG can be described by the Hamiltonian

$$H_{\alpha s} = - \sum_{\mathbf{k}} (\Delta_{\alpha} e^{i\phi_{\alpha}} c_{\alpha\mathbf{k}\uparrow}^{\dagger} c_{\alpha-\mathbf{k}\downarrow}^{\dagger} + \text{H.c.}), \quad (3)$$

with a phase ϕ_{α} of the order parameter Δ_{α} . With the aids of RSOC, the spin-singlet s -wave order parameter effectively generates the spin-triplet p -wave pairing states in the 2DEG [31,32]. The out-of-plane Zeeman splitting

$$H_{\alpha z} = \sum_{\mathbf{k}\sigma} \sigma_z V_{\alpha z} c_{\alpha\mathbf{k}\sigma}^{\dagger} c_{\alpha\mathbf{k}\sigma} \quad (4)$$

inherited from the ferromagnetic insulator significantly influences the pairing states, and $\sigma_z = \pm 1$ corresponds to $\sigma (= \uparrow, \downarrow)$. The Hamiltonian of the QD is

$$H_{QD} = \sum_{\sigma} \varepsilon_{d\sigma} d_{\sigma}^{\dagger} d_{\sigma} + U n_{\uparrow} n_{\downarrow}, \quad (5)$$

with the dot level $\varepsilon_{d\sigma}$ and the Coulomb repulsion U . d_{σ}^{\dagger} (d_{σ}) is the creation (annihilation) operator of dot electrons and $n_{\sigma} = d_{\sigma}^{\dagger} d_{\sigma}$. The coupling between the dot and the superconducting leads is

$$H_V = \sum_{\alpha k \sigma} (V_{\alpha} c_{\alpha k \sigma}^{\dagger} d_{\sigma} + \text{H.c.}), \quad (6)$$

where the coupling amplitude V_{α} is assumed to be independent of the spin and momentum. The transport through the junction can be used to discuss the physics dominated by the interaction between the dot spin and the mixed s -wave and p -wave pairing states in the 2DEG.

To treat the Hamiltonian of the 2DEG (H_{α}) in the leads, it is natural to introduce the angular momentum basis,

$$c_{\alpha k \sigma} = \sqrt{\frac{2\pi}{k}} \sum_{m=-\infty}^{\infty} e^{im\theta_k} c_{\alpha k \sigma}^m, \quad (7)$$

where m is the quantum number of orbital angular momentum, and the operator $c_{\alpha k \sigma}^{m\dagger}$ ($c_{\alpha k \sigma}^m$) satisfies the canonical anticommutation relationship. In the presence of RSOC, the Hamiltonian is not diagonal due to the coupling between spin and orbital degrees of freedom, while the z component of total angular momentum, $j_z = m + \sigma_z/2$, is still a conserved quantity [39–42]. It is convenient to perform a canonical transformation to introduce the fermionic operators, such as

$$\tilde{c}_{\alpha h k m+1/2} = \frac{1}{\sqrt{2}} (\beta_{\alpha h k} c_{\alpha k \uparrow}^m + h \beta_{\alpha -h k} c_{\alpha k \downarrow}^{m+1}), \quad (8)$$

with $\beta_{\alpha h k} = (1 + hV_{\alpha z}/\sqrt{\lambda_{\alpha}^2 k^2 + V_{\alpha z}^2})^{1/2}$, and $h = \pm 1$ is the chirality quantum number [41,42]. These fermionic operators satisfy the anticommutation relationship

$$[\tilde{c}_{\alpha h k m+1/2}, \tilde{c}_{\alpha h' k' m'+1/2}]_{\pm} = \delta(k - k') \delta_{h'h} \delta_{m'm}. \quad (9)$$

After some straightforward calculations (see the details in the Appendix), the Hamiltonian of the 2DEG can be written as

$$H_{\alpha} = \sum_{h j} \int dk \varepsilon_{\alpha h k} \tilde{c}_{\alpha h k j}^{\dagger} \tilde{c}_{\alpha h k j} - \frac{\Delta_{\alpha}}{2} \sum_{h'h} \int dk \times (h \beta_{\alpha -h k} \beta_{\alpha h' k} \tilde{c}_{\alpha h k 1/2}^{\dagger} \tilde{c}_{\alpha h' -k -1/2}^{\dagger} + \text{H.c.}), \quad (10)$$

with $\varepsilon_{\alpha h k} = \varepsilon_{\alpha k} + h\sqrt{\lambda_{\alpha}^2 k^2 + V_{\alpha z}^2}$ and $j = m + \sigma$. Here, the superconducting pairing interaction term includes the interband ($h = -h'$) s -wave pairing and the intraband ($h = h'$) p -wave pairing components [43–45]. The hybridization between the dot level and leads can be rewritten as

$$H_V = \sum_{\alpha h j} \int dk \tilde{V}_{\alpha} (h^{-j+1/2} \beta_{\alpha \text{sign}(j) h k} \tilde{c}_{\alpha h k j}^{\dagger} d_j + \text{H.c.}), \quad (11)$$

with $\tilde{V}_{\alpha} = \sqrt{k/8\pi} V_{\alpha}$, and the sign function $\text{sign}(j) = \pm 1$ for $j_z = \pm 1/2$. Here, we consider the short-range scattering, and the dot spin is coupled only to the conduction electrons with $m = 0$. Then, we note the operator $d_{\sigma} \rightarrow d_j$ and rewrite the dot level $\varepsilon_{d\sigma} \rightarrow \varepsilon_j$.

In the present work, we treat the Hamiltonian of the junction by the equation-of-motion (EOM) approach. In frequency space, the dot Green's function (GF) in the Nambu representation reads

$$\hat{G}_j(\omega) = \hat{G}_j^0(\omega) [1 + U \hat{F}_{d_j}(\omega)], \quad (12)$$

where $\hat{G}_j(\omega) = \langle\langle \hat{\Psi}_j; \hat{\Psi}_j^{\dagger} \rangle\rangle$ with $\hat{\Psi}_j^{\dagger} = (d_j^{\dagger}, d_{-j})$, and

$$\hat{G}_j^0(\omega) = [\hat{I}\omega - \hat{\sigma}_z \text{diag}(\varepsilon_j, \varepsilon_{-j}) - \hat{\Sigma}_j^0(\omega)]^{-1} \quad (13)$$

is the noninteracting GF. The components of the noninteracting self-energy $\hat{\Sigma}_j^0(\omega)$ are

$$\hat{\Sigma}_{j11(22)}^0(\omega) = \frac{1}{\pi} \sum_{\alpha h} \int d\varepsilon_{\alpha h k} \Gamma_{\alpha h j}(\varepsilon_{\alpha h k}) \Pi_{\alpha h j 11(22)}(\omega, \varepsilon_{\alpha h k}) \quad (14)$$

and

$$\hat{\Sigma}_{j12(21)}^0(\omega) = \frac{1}{\pi} \sum_{\alpha h} \int d\varepsilon_{\alpha h k} \Gamma_{\alpha h j}(\varepsilon_{\alpha h k}) \Pi_{\alpha h j 11(22)}(\omega, \varepsilon_{\alpha h k}) \times \Omega_{\alpha h j 11(22)}(\omega, \varepsilon_{\alpha h k}), \quad (15)$$

where the notations are $\Pi_{\alpha h j 11(22)}(\omega, \varepsilon_{\alpha h k}) = \beta_{\alpha \text{sign}(j) h k}^2 [\omega \mp \varepsilon_{\alpha h k} - \frac{\Delta_{\alpha}^2 \xi_{\alpha h k \mp j}}{4} (\frac{\beta_{\alpha \text{sign}(+j) h k}^2}{\omega \pm \varepsilon_{\alpha h - k}} + \frac{\beta_{\alpha \text{sign}(+j) h k}^2}{\omega \pm \varepsilon_{\alpha - h - k}})]^{-1}$ with $\xi_{\alpha h k j} = \beta_{\alpha \text{sign}(j) h k}^2 + \beta_{\alpha \text{sign}(j) h k} \beta_{\alpha \text{sign}(-j) h k}$ and $\Omega_{\alpha h j 11(22)}(\omega, \varepsilon_{\alpha h k}) = \beta_{\alpha \text{sign}(-j) h k}^2 (\frac{1}{\omega \pm \varepsilon_{\alpha h - k}} - \frac{1}{\omega \pm \varepsilon_{\alpha - h - k}})$. The coupling strength can be evaluated as $\Gamma_{\alpha h j}(\varepsilon_{\alpha h k}) = \Gamma_{0\alpha} \rho_{\alpha h j}(\varepsilon_{\alpha h k})$ with $\Gamma_{0\alpha} = \pi |V_{\alpha}|^2 / 2D_{\alpha}$, where D_{α} is the half-band width of the leads. The density of states can be expressed as

$$\rho_{\alpha h j}(\varepsilon_{\alpha h k}) = \begin{cases} \frac{m}{8\pi h^2} \frac{\varepsilon_{\alpha R} - \text{sign}(j) V_{\alpha z}}{2\sqrt{\varepsilon_{\alpha R}(\varepsilon_{\alpha h k} - \tilde{\varepsilon}_{\alpha 0})}} \Theta(2\varepsilon_{\alpha R} - V_{\alpha z}) \delta_{h,-1}; & \tilde{\varepsilon}_{\alpha 0} < \varepsilon_{\alpha h k} < E_{\alpha 0} - V_{\alpha z}, \\ \frac{m}{8\pi h^2} (\frac{1}{2} - h \frac{\varepsilon_{\alpha R} - \text{sign}(j) V_{\alpha z}}{2\sqrt{\varepsilon_{\alpha R}(\varepsilon_{\alpha h k} - \tilde{\varepsilon}_{\alpha 0})}}); & E_{\alpha 0} + hV_{\alpha z} < \varepsilon_{\alpha h k} < D_{\alpha h}, \\ 0 & \text{otherwise,} \end{cases} \quad (16)$$

where $D_{\alpha h} = D_{\alpha} + 2h\sqrt{(D_{\alpha} - E_{\alpha 0} + V_{\alpha z}^2/4\varepsilon_{\alpha R})\varepsilon_{\alpha R}}$ and $\tilde{\varepsilon}_{\alpha 0} = E_{\alpha 0} - V_{\alpha z}^2/4\varepsilon_{\alpha R} - \varepsilon_{\alpha R}$. $\varepsilon_{\alpha R} = m\lambda_{\alpha}^2/2$ denotes the energy of RSOC. $E_{\alpha 0}$ is the bottom of the conduction band in the absence of RSOC.

The notation $\hat{F}_{d_j}(\omega)$ includes some high-order GFs. However, it is difficult to exactly calculate these GFs by theoretical treatments [46–49]. In the present work, we treat these high-order GFs by using the EOM approach [50–60]. Here, we

pay attention to the competition between the Kondo effect and the mixed s -wave and p -wave pairing states in the leads. Thus, we truncate the diagonal components of $\hat{F}_{dj}(\omega)$ with the Lacroix approximation scheme [22,50,61]. It is believed to qualitatively capture the Kondo effect even at zero temperature [51,54–56]. Based on the theoretical treatment as shown in the Appendix, we obtain the dot GF,

$$\hat{G}_j(\omega)_{11} = \frac{1 + UO_j(\omega) + [1 + UP_j(\omega)]\hat{\Sigma}_{j21}^0\hat{G}_j(\omega)_{21}}{\omega - \varepsilon_j - \hat{\Sigma}_{j11}^0(\omega) - U[P_j(\omega) - Q_j(\omega)]}, \quad (17)$$

where $O_j(\omega) = [\langle n_{-j} \rangle + A_{j1}(\omega) - A_{j2}(\omega)]/M_j(\omega)$, $P_j(\omega) = [A_{j1}(\omega) - A_{j2}(\omega)]\hat{\Sigma}_{j11}^0(\omega)/M_j(\omega)$, and $Q_j(\omega) = [B_{j1}(\omega) + B_{j2}(\omega)]/M_j(\omega)$ with $M_j(\omega) = \omega - \varepsilon_j - U - \Xi_{j0}(\omega) - \Xi_{j1}(\omega) - \Xi_{j2}(\omega)$, and $\Xi_{j0}(\omega) = \frac{1}{\pi} \sum_{\alpha h} \int d\varepsilon_{\alpha hk} \frac{\Gamma_{\alpha hj}(\varepsilon_{\alpha hk})\beta_{\alpha \text{sign}(j)hk}^2}{\omega - \varepsilon_{\alpha hk} + i0^+}$. The occupation of the dot level is $\langle n_j \rangle = -\frac{1}{\pi} \int f(\omega)\text{Im}[\hat{G}_j(\omega)_{11}]d\omega$, and $f(\omega)$ is the Fermi distribution function. Other notations can be expressed as

$$\Xi_{j\eta}(\omega) = \frac{1}{\pi} \sum_{\alpha h} \int d\varepsilon_{\alpha hk} \frac{\Gamma_{\alpha hj}(\varepsilon_{\alpha hk})\beta_{\alpha \text{sign}(j)hk}^2}{\omega - \varepsilon_{\eta\alpha hk} + i0^+}, \quad (18)$$

$$A_{j\eta}(\omega) = \frac{i}{\pi^2} \sum_{\alpha h} \int d\varepsilon_{\alpha hk} \frac{\Gamma_{\alpha hj}(\varepsilon_{\alpha hk})\Theta_{\alpha hj}(\varepsilon_{\alpha hk})}{\omega - \varepsilon_{\eta\alpha hk} + i0^+}, \quad (19)$$

$$B_{j\eta}(\omega) = \frac{i}{\pi^2} \sum_{\alpha h} \int d\varepsilon_{\alpha hk} \frac{\Gamma_{\alpha hj}(\varepsilon_{\alpha hk})\Lambda_{\alpha hj}(\varepsilon_{\alpha hk})}{\omega - \varepsilon_{\eta\alpha hk} + i0^+}, \quad (20)$$

with $\eta = 1, 2$. In these notations, $\Theta_{\alpha hj}(\varepsilon_{\alpha hk}) = \int f(\omega)(\omega + \varepsilon_{\alpha hk})\Pi_{\alpha h-j11}(\omega, \varepsilon_{\alpha hk})\hat{G}_j(\omega)_{11}d\omega$ and $\Lambda_{\alpha hj}(\varepsilon_{\alpha hk}) = \int f(\omega)(\omega + \varepsilon_{\alpha hk})\Pi_{\alpha h-j11}(\omega, \varepsilon_{\alpha hk})d\omega$. The symbols are $\varepsilon_{1\alpha hk} = \varepsilon_j - \varepsilon_{-j} + \varepsilon_{\alpha hk}$, $\varepsilon_{2\alpha hk} = -\varepsilon_{\alpha hk} + \varepsilon_{-j} + \varepsilon_j + U$. Here, we would like point out that the superconducting correlation on the dot level is significantly suppressed by the large Coulomb repulsion due to $U \gg \Delta_\alpha$. Therefore, the Hartree-Fock approximation (HFA) in the off-diagonal parts of $\hat{F}_{dj}(\omega)$ is good enough [22,61–63]. We can conveniently obtain the anomalous GF of the QD,

$$\hat{G}_j(\omega)_{21} = \frac{U\langle d_j^\dagger d_{-j}^\dagger \rangle - \hat{\Sigma}_{j21}^0(\omega)}{\omega + \varepsilon_{-j} - \hat{\Sigma}_{j22}^0(\omega) + U\langle n_j \rangle} \hat{G}_j(\omega)_{11}. \quad (21)$$

The superconducting pairing correlation can be evaluated with $\langle d_j^\dagger d_{-j}^\dagger \rangle = -\frac{1}{\pi} \int f(\omega)\text{Im}[\hat{G}_j(\omega)_{21}]d\omega$. The dot GF's described by Eqs. (17) and (21) can be calculated self-consistently with the above formulas. The Josephson current through the QD is

$$J_c(\phi) = \frac{4e}{\hbar\pi} \sum_{hh'} \int d\omega \sin(\phi/2)\Gamma_{Rh_j}(\omega)f(\omega) \times \text{Im}\{hF_{h'h}(\omega)[\hat{G}_{-j}(\omega)_{21} - h'\hat{G}_j(\omega)_{21}]\}, \quad (22)$$

with the superconducting phase $\phi_R = -\phi_L = \phi/2$, and the notation $F_{h'h}(\omega) = \frac{\Delta_R}{2} \frac{1}{(\omega - \varepsilon_{Rh}) (\omega + \varepsilon_{Rh'}) - \Delta_R^2 g_{Rh}(\omega)}$ with $g_{Rh}(\omega) = \frac{\omega^2 - \varepsilon_{Rh}^2}{\omega^2 - \varepsilon_{R-hk}^2}$. The Josephson current is mainly determined by the spin-induced YSR state in the mixed s -wave and p -wave pairing states [31,32,44,45].

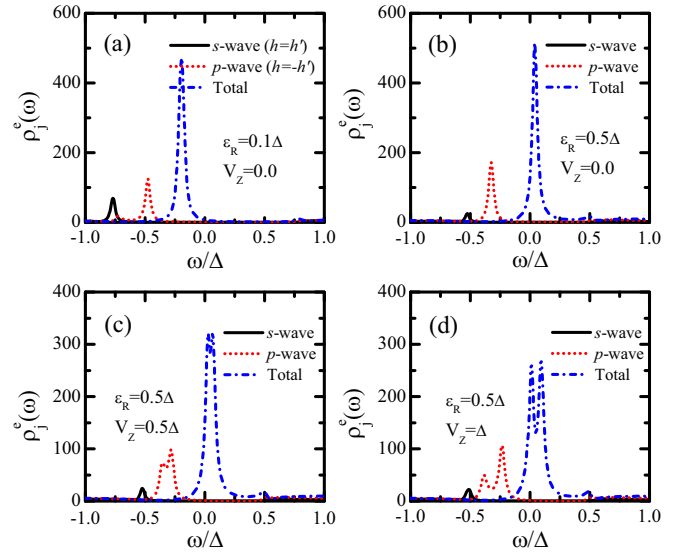


FIG. 2. Electron part of spin-induced Yu-Shiba-Rusinov (YSR) state in the mixed s -wave ($h = h'$) and p -wave ($h = -h'$) pairing states in the presence of RSOC with (a) $\varepsilon_R = 0.1\Delta$ and (b) $\varepsilon_R = 0.5\Delta$ shown as the blue dash-dotted line (Total) in the local density of states (LDOS). The YSR states induced separately in the s -wave and p -wave pairing components are shown by the black solid and red dotted lines, respectively. The hole part of the YSR state is neglected due to the electron-hole symmetry. The Zeeman field splits the YSR state induced in the spin-triplet states shown by the red dotted lines in (c) $V_Z = 0.5\Delta$ and (d) $V_Z = \Delta$. The parameters are the dot level $\varepsilon_{d\sigma} = -7.5\Delta$, the Coulomb repulsion $U = 200\Delta$, the coupling strength $\Gamma_0 = 1.25\Delta$, the temperature $T = 0$, and the chemical potentials $\mu = 0$.

III. NUMERICAL RESULTS

RSOC breaks the $SU(2)$ spin-rotation symmetry and creates the spin-triplet pairing states in the 2DEG with the proximity-induced pairing interaction [31,32,36,38,43,45]. The spin-induced YSR states are qualitatively different in the s -wave and p -wave superconductors due to the discrepancies in the superconducting pairing symmetry [38]. Here, we focus on the Kondo screening of the dot spin coupled to the leads with mixed s -wave and effective p -wave pairing states. If it is not explicitly mentioned, we assume the QD is symmetrically coupled with the superconducting leads by setting $\Delta_\alpha = \Delta$, $\varepsilon_{\alpha R} = \varepsilon_R$, $V_{\alpha z} = V_z$, $\Gamma_{0\alpha} = \Gamma_0$, and $\mu_\alpha = \mu$ for simplification. All the parameters are measured in units of the energy gap Δ .

In order to discuss the Kondo effect originating from the s -wave and p -wave pairing components separately, we consider the self-energies contributed from the interband ($h = h'$) s -wave pairing and the intraband ($h = -h'$) p -wave pairing states, respectively. Then, we obtain the spin-induced YSR states in the s -wave and p -wave pairing components marked by the black solid and red dotted lines in Figs. 2(a)–2(d), respectively. By increasing RSOC ε_R , the YSR state, denoted by the solid lines in Figs. 2(a) and 2(b), is significantly suppressed due to the decrease of the s -wave pairing component in the 2DEG. Oppositely, the increase of p -wave pairing components results in the enhancement of YSR states, as shown by the red dotted lines. By taking account of all the

contributions of the s -wave and p -wave pairing components, the Kondo screening of the dot spin is enhanced by increasing the RSOC, as indicated by the level position of the YSR states (see the blue dash-dotted lines) [18]. Here, we merely plot the electron part of the YSR state in the local density of states (LDOS), $\rho_j^e(\omega) = -\frac{1}{\pi} \text{Im} \Sigma_j \hat{G}_j(\omega)_{11}$, because the hole part of the YSR state would be symmetrically posited about the Fermi level due to particle-hole symmetry [18–20]. In the presence of Zeeman field V_z in the 2DEG, the YSR state is split, as shown in the blue dash-dotted lines in Figs. 2(c) and 2(d). The spin degeneracy of the doublet formed by the excitations in the triplet states, such as $(1 \downarrow)$ and $(-1 \uparrow)$ [see Fig. 1(a)], has been removed by the Zeeman energy. Therefore, the YSR state induced in the spin-triplet states shows splitting marked by the red dotted lines. The Zeeman splitting in the leads does not affect the YSR state induced in the s -wave component. Here, we ignore the effect of the Zeeman field on the orbital degrees of freedom for simplification [31,32].

The subgap transport of the junction is determined by the interplay between the Kondo effect and the superconducting pairing states at low temperatures. In the absence of the Zeeman field ($V_z = 0$), RSOC leads to the level-crossing QPT, which indicates that RSOC plays a role in enhancing the Kondo screening of the dot spin shown in Fig. 3(a) [18]. This is because RSOC not only enhances the Kondo screening of a local moment in a normal metal [39,41,42], but also introduces a new Kondo screening channel of the magnetic moment in a superconductor [22]. The RSOC-induced level-crossing QPT between the magnetic doublet and Kondo singlet ground states takes place about $\varepsilon_R = 0.35\Delta$. Correspondingly, the Josephson current $J_c(\phi)$ displays a $0-\pi$ phase transition marked by the blue dotted line in Fig. 3(b). The $0-\pi$ phase transition of the Josephson current is a good candidate to detect the ground states QPT of the QD coupled with superconducting leads [14,15,17].

Taking account of the Zeeman field inherent from the ferromagnetic insulator, the YSR state is split by the increase of V_z as shown in Figs. 3(c) and 3(e). The Zeeman splitting removes the spin degeneracy of the doublet formed by the excitations in triplet states. Note that the YSR cannot be split by the Zeeman energy in the absence of RSOC because the Zeeman field does not break the spin-rotation symmetry of the 2DEG. In Fig. 3(d), the Josephson current through the junction shows the $0-\pi$ phase transition at $V_z = 2.35\Delta$. Accordingly, the QPT between the Kondo singlet and magnetic doublet states is accompanied by one branch of the split YSR states crossing the Fermi level marked by the dash-dotted line in Fig. 3(c) [17]. In Fig. 3(e), the ground state is a magnetic doublet even in the absence of Zeeman energy. The Josephson current is always in the π phase and suppressed by the Zeeman-induced splitting of the YSR state, as shown in Fig. 3(f).

As we have mentioned above, the YSR state and the Josephson current directly reflect the interplay of the local moment and p -wave pairing states under the Zeeman field V_z . In Fig. 4(a), we show the splitting of the YSR state depending on the lead-dot coupling. The Kondo screening is enhanced by increasing the coupling strength Γ_0 , and the YSR state is tuned getting close to the Fermi level. Meanwhile, the

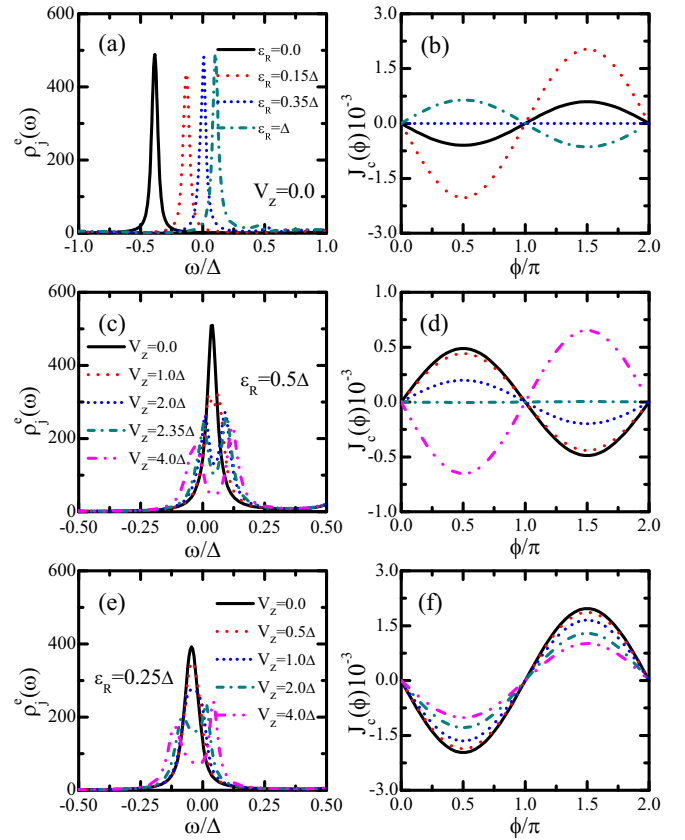


FIG. 3. (a) The level-crossing QPT driven by RSOC leads to a $0-\pi$ phase transition in the Josephson current (b). (c), (e) The splitting of the YSR state by increasing the Zeeman splitting V_z . (d) The Josephson current displays a $0-\pi$ phase transition behavior if the ground state is a Kondo singlet with $\varepsilon_R = 0.5\Delta$. (f) The Josephson current is suppressed by increasing the Zeeman energy whenever the ground state is a magnetic doublet with $\varepsilon_R = 0.25\Delta$. Other parameters used are the same as that in Fig. 2.

splitting of the YSR state is enlarged due to the increase of coupling between the dot spin and spin-triplet pairing states. In Fig. 4(b), we show the spin dependence of the YSR states, which directly reflects the breaking of spin degeneracy of the doublet state formed by excitations. The splitting of the YSR state can be eliminated by aligning the orientation of the ferromagnetic insulator of the leads oppositely ($V_{Lz} = -V_{Rz}$), as shown in Fig. 4(c). In addition, the Kondo screening of a local moment can be observed from the magnetic susceptibility, $\chi_d(T) = \frac{g\mu_B(n_{\uparrow} - n_{\downarrow})}{h} |_{h \rightarrow 0}$, as shown in Fig. 4(d), and we take $g = \mu_B = 1$. The temperature dependence of $\chi_d(T)$ indicates that the Kondo effect exists even in the presence of a large Zeeman field. However, a complete Kondo screened singlet state cannot be realized in triplet states with the breaking of time-reversal symmetry. This result agrees with that obtained by the numerical renormalization-group calculations [24,25,29]. Intuitively, the microscopic processes underlying the Kondo effect in triplet states, as shown in Figs. 1(b)–1(f), suggest that the complete screening of the local moment cannot be realized due to the spin polarization in the doublet state formed in triplet states.

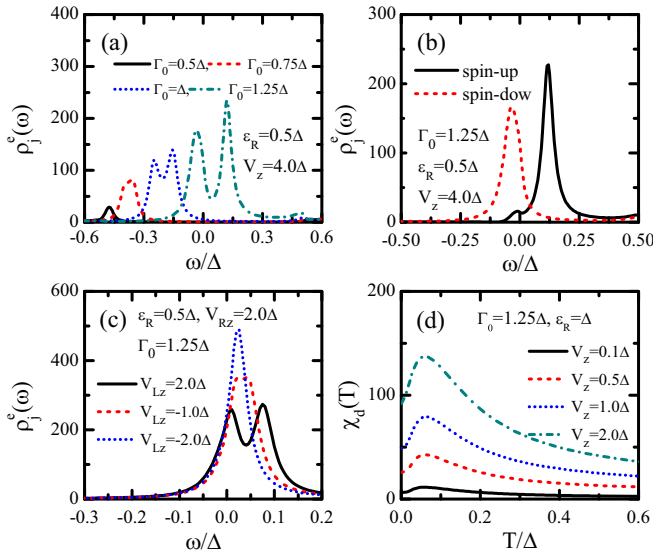


FIG. 4. (a) The splitting of the YSR state in a QD symmetrically coupled with the superconducting leads with RSOC $\varepsilon_R = 0.5\Delta$ and the Zeeman energy $V_z = 4\Delta$. (b) The spin-dependent splitting of the YSR state in (a) with $\Gamma_0 = 1.25\Delta$. (c) Elimination of the splitting of the YSR state by orienting the magnetization of the ferromagnetic insulators oppositely with $V_{Lz} = -V_{Rz}$, where the minus (-) indicates the opposite magnetization directions. (d) The Zeeman-dependent magnetic susceptibility varying with the temperature T with $\varepsilon_R = \Delta$. Other parameters used are the same as that in Fig. 2.

IV. CONCLUSION AND DISCUSSION

In this work, we studied the Kondo screening of a dot spin coupled to the superconducting leads with spin-triplet p -wave pairing states. Taking account of short-range scattering, only the conduction electrons with $m = 0$ contribute to the Kondo effect, and the excitations with $m = \pm 1$ form a spin-doublet state in the energy gap. In addition, the Kondo screening involves the orbital angular momentum conserved transitions between the p -wave pairing states. The Zeeman field inherent from the ferromagnet removes the spin degeneracy of quasiparticle excitations. As a result, the YSR state exhibits Zeeman-dependent splitting behaviors. The splitting of the YSR state leads to a 0 - π phase transition or the suppression of the Josephson current, depending on the ground states of the system. The temperature-dependent behaviors of magnetic susceptibility indicate that the local moment should be partially screened due to the spin polarization in the excitations in the triplet states. In Ref. [22], the QPT between the magnetic doublet and the Kondo singlet ground states is matched by a phenomenological model that gives rise to the Rashba-induced quantum state transition (QST) of conduction electrons. Actually, the QSTs are closely related to the creation of spin-triplet states. The present system allows us to directly investigate the effect of spin-triplet states on the Kondo screening. The spin-triplet states manifest themselves in the splitting of the YSR states under the Zeeman field caused by ferromagnets.

In the last decade, similar devices have been theoretically proposed to study the interplay between the Kondo effect and Majorana zero mode (MZM) [29,64–72]. In these cases,

the Kondo resonance shows splitting [64–66], and the Kondo fixed point cannot be reached due to the presence of MZM [67,72]. The MZM is a coherent superposition of electrons and holes from the same spin band [73–76]. Thus, the splitting of Kondo resonance [64–66] directly reflects the Ising property of the Majorana end state [77–79]. For our purpose, we focus on the bulk states of the setup and thus neglect the MZMs. Therefore, the behaviors of the YSR states are determined by the competition between the Kondo effect and the p -wave pairing states in the 2DEG.

ACKNOWLEDGMENTS

We are grateful to Professor Hong Guo and Professor Hao-Ran Chang for helpful discussions. This work was supported by the NSFC (under Grants No. 12074108, No. 11704106, No. 11874273, No. 11834005, No. 11861161001, No. 11904234, and No. 11904245), the Project of Sichuan Science and Technology Program (Grants No. 2019YFSY0044 and No. 2020YJ0136), and Zhejiang Provincial Natural Science Foundation of China (Grant No. LY19A040003).

APPENDIX

In this Appendix, we outline the procedures to obtain the simplified Hamiltonian [see Eq. (10)] of the two-dimensional electron gas (2DEG) in the leads. Then, we present the main steps to obtain the dot Green's function (GF) of the hybrid superconductor-QD junction with mixed s -wave and p -wave superconducting pairing states.

To treat the Hamiltonian of the 2DEG H_α in Eq. (1), it is convenient to introduce the angular momentum basis of the conduction electrons,

$$c_{\alpha k \sigma} = \sqrt{\frac{2\pi}{k}} \sum_{m=-\infty}^{\infty} e^{im\theta_k} c_{\alpha k \sigma}^m. \quad (\text{A1})$$

The operators satisfy the canonical anticommutation relation,

$$[c_{\alpha k \sigma}^m; c_{\alpha k' \sigma'}^{m'\dagger}]_+ = \delta(k - k') \delta_{\sigma \sigma'} \delta_{mm'}. \quad (\text{A2})$$

By transferring the summation of the in-plane vector \mathbf{k} into the integration of k , such as $\sum_{\mathbf{k}} = \frac{1}{4\pi^2} \int k dk d\theta_k$, we obtain

$$\begin{aligned} H_\alpha = & \sum_m \int dk (\varepsilon_{\alpha k} + \sigma_z \varepsilon_{\alpha z}) c_{\alpha k \sigma}^{m\dagger} c_{\alpha k \sigma}^m \\ & + \sum_m \int dk \lambda_{\alpha k} (c_{\alpha k \downarrow}^{(m+1)\dagger} c_{\alpha k \uparrow}^m + \text{H.c.}) \\ & - \Delta_\alpha \sum_m \int dk (c_{\alpha k \uparrow}^{m\dagger} c_{\alpha -k \downarrow}^{-m\dagger} + \text{H.c.}). \end{aligned} \quad (\text{A3})$$

In order to diagonalize the Rashba term, one can take a canonical transformation of the fermionic operators in Eq. (A3),

$$c_{\alpha h k m+1/2} = \frac{1}{\sqrt{2}} (\beta_{\alpha h k} c_{\alpha k \uparrow}^m + h \beta_{\alpha -h k} c_{\alpha k \downarrow}^{m+1}), \quad (\text{A4})$$

with $\beta_{\alpha h k} = (1 + hV_{\alpha z} / \sqrt{\lambda_{\alpha k}^2 k^2 + \varepsilon_{\alpha z}^2})^{1/2}$, and $h = \pm 1$ is the chirality quantum number. These fermionic operators satisfy the canonical anticommutation relationship,

$$[c_{\alpha h k m+1/2}, c_{\alpha h' k' m'+1/2}^\dagger]_+ = \delta(k - k') \delta_{h' h} \delta_{m', m}. \quad (\text{A5})$$

Then, we obtain

$$H_\alpha = \sum_{hm} \int dk \varepsilon_{\alpha hk} c_{\alpha hkm+1/2}^\dagger c_{\alpha hkm+1/2} - \frac{\Delta_\alpha}{2} \sum_{hh'm} \int dk (\beta_{\alpha-hk} \beta_{\alpha h'k} h c_{\alpha hkm-1/2}^\dagger c_{\alpha h'-k-m+1/2}^\dagger + \text{H.c.}), \quad (\text{A6})$$

with $\varepsilon_{\alpha hk} = \varepsilon_{\alpha k} + h\sqrt{\lambda_\alpha^2 k^2 + \varepsilon_{\alpha z}^2}$. In the presence of RSOC, the spin and orbital angular momentum are not conserved, while the total angular momentum $j = m + \sigma$ is a conserved quantity. The Hamiltonian of the hybrid coupling between the QD and leads can be rewritten as

$$H_V = \sum_{\alpha h j} \int dk \tilde{V}_\alpha (h^{-j+1/2} \beta_{\alpha \text{sign}(j)hk} c_{\alpha hk}^\dagger d_j + \text{H.c.}), \quad (\text{A7})$$

with $\tilde{V}_\alpha = \sqrt{k/8\pi} V_\alpha$. Here, we denote $d_\sigma^\dagger (d_\sigma) \rightarrow d_j^\dagger (d_j)$ as the creation (annihilation) of an electron on the dot level, and the z component of the total angular momentum is $j_z = \pm 1/2$. Thus, the Hamiltonian of the junction can be read,

$$H = \sum_{\alpha h j} \int dk \varepsilon_{\alpha hk} c_{\alpha hk}^\dagger c_{\alpha hk} + \sum_j \varepsilon_j d_j^\dagger d_j + U n_\uparrow n_\downarrow - \sum_{\alpha h h' j} \int dk \frac{\Delta_\alpha}{2} (\beta_{\alpha-hk} \beta_{\alpha h'k} h c_{\alpha hk}^\dagger c_{\alpha h'-k-j}^\dagger + \text{H.c.}) \\ + \sum_{\alpha h j} \int dk \tilde{V}_\alpha (h^{-j+1/2} \beta_{\alpha \text{sign}(j)hk} c_{\alpha hk}^\dagger d_j + \text{H.c.}). \quad (\text{A8})$$

The RSOC leads to an indirect exchange coupling between the dot spin and the conduction electrons with different spin and orbital states [41,42]. Here, we just consider the short-range scattering, and the dot spin is coupled only to the conduction electrons with $m = 0$ [24,25,27,29].

In the present work, we treat the Hamiltonian described by Eq. (A8) based on the EOM approach [50,51,56]. The start point is the EOM of the retarded GF,

$$\omega \langle \langle A; B \rangle \rangle = \langle [A, B]_+ \rangle + \langle \langle [A, H]_-; B \rangle \rangle, \quad (\text{A9})$$

composed of the operators A and B , where the subscript \pm stands for the anticommutation (commutation) relationship [80]. Here, the EOMs of the retarded GFs composed of the creation and annihilation operators of the localized and itinerant electrons read

$$\omega \langle \langle d_j; B \rangle \rangle = \langle [d_j; B]_+ \rangle + \varepsilon_j \langle \langle d_j; B \rangle \rangle + U \langle \langle d_j n_{-j}; B \rangle \rangle + \sum_{\alpha h} \int dk \tilde{V}_\alpha h^{-j+1/2} \beta_{\alpha \text{sign}(j)hk} \langle \langle c_{\alpha hk}; B \rangle \rangle \quad (\text{A10})$$

and

$$\omega \langle \langle d_j^\dagger; B \rangle \rangle = \langle [d_j^\dagger; B]_+ \rangle - \varepsilon_j \langle \langle d_j^\dagger; B \rangle \rangle - U \langle \langle d_j^\dagger n_{-j}; B \rangle \rangle - \sum_{\alpha h} \int dk \tilde{V}_\alpha h^{-j+1/2} \beta_{\alpha \text{sign}(j)hk} \langle \langle c_{\alpha hk}^\dagger; B \rangle \rangle, \quad (\text{A11})$$

$$\omega \langle \langle c_{\alpha hk}; B \rangle \rangle = \langle [c_{\alpha hk}; B]_+ \rangle + \varepsilon_{\alpha hk} \langle \langle c_{\alpha hk}; B \rangle \rangle + h^{-j+1/2} \tilde{V}_\alpha \beta_{\alpha \text{sign}(j)hk} \langle \langle d_j; B \rangle \rangle \\ - \delta_{j,1/2} \frac{\Delta_\alpha}{2} \sum_{h'} h \beta_{\alpha-hk} \beta_{\alpha h'k} \langle \langle c_{\alpha h'-k-1/2}^\dagger; B \rangle \rangle + \delta_{j,-1/2} \frac{\Delta_\alpha}{2} \sum_{h'} h' \beta_{\alpha-h'k} \beta_{\alpha hk} \langle \langle c_{\alpha h'-k-1/2}^\dagger; B \rangle \rangle, \quad (\text{A12})$$

$$\omega \langle \langle c_{\alpha hk}^\dagger; B \rangle \rangle = \langle [c_{\alpha hk}^\dagger; B]_+ \rangle - \varepsilon_{\alpha hk} \langle \langle c_{\alpha hk}^\dagger; B \rangle \rangle - h^{-j+1/2} \tilde{V}_\alpha \beta_{\alpha \text{sign}(j)hk} \langle \langle d_j^\dagger; B \rangle \rangle \\ + \delta_{j,1/2} \frac{\Delta_\alpha}{2} \sum_{h'} h \beta_{\alpha-hk} \beta_{\alpha h'k} \langle \langle c_{\alpha h'-k-1/2}; B \rangle \rangle - \delta_{j,-1/2} \frac{\Delta_\alpha}{2} \sum_{h'} h' \beta_{\alpha-h'k} \beta_{\alpha hk} \langle \langle c_{\alpha h'-k-1/2}; B \rangle \rangle. \quad (\text{A13})$$

By some straightforward calculations and choosing the operator $B = d_j^\dagger$ or d_{-j} , we obtain the dot GFs expressed in the Nambu representation,

$$\begin{pmatrix} \omega - \varepsilon_j - \hat{\Sigma}_{j11}^0(\omega) & \hat{\Sigma}_{j12}^0(\omega) \\ \hat{\Sigma}_{j21}^0(\omega) & \omega + \varepsilon_{-j} - \hat{\Sigma}_{j22}^0(\omega) \end{pmatrix} \begin{pmatrix} \langle \langle d_j; d_j^\dagger \rangle \rangle & \langle \langle d_j; d_{-j} \rangle \rangle \\ \langle \langle d_{-j}^\dagger; d_j^\dagger \rangle \rangle & \langle \langle d_{-j}^\dagger; d_{-j} \rangle \rangle \end{pmatrix} = \begin{pmatrix} 1 & 0 \\ 0 & 1 \end{pmatrix} + U \begin{pmatrix} \langle \langle d_j n_{-j}; d_j^\dagger \rangle \rangle & \langle \langle d_j n_{-j}; d_{-j} \rangle \rangle \\ -\langle \langle d_{-j}^\dagger n_j; d_j^\dagger \rangle \rangle & -\langle \langle d_{-j}^\dagger n_j; d_{-j} \rangle \rangle \end{pmatrix}, \quad (\text{A14})$$

where the noninteracting self-energy terms are

$$\hat{\Sigma}_{j11(22)}^0(\omega) = \frac{1}{\pi} \sum_{h\alpha} \int \frac{d\varepsilon_{\alpha hk} \Gamma_{\alpha h j} (\varepsilon_{\alpha hk}) \beta_{\alpha \text{sign}(\pm j)hk}^2}{\omega \mp \varepsilon_{\alpha hk} - \frac{\Delta_\alpha}{4} \xi_{\alpha h \pm jk} \left(\frac{\beta_{\alpha \text{sign}(\pm j)hk}^2}{\omega \pm \varepsilon_{\alpha-hk}} + \frac{\beta_{\alpha \text{sign}(\mp j)hk}^2}{\omega \pm \varepsilon_{\alpha-hk}} \right)}, \quad (\text{A15})$$

and the off-diagonal elements are

$$\hat{\Sigma}_{j12(21)}^0(\omega) = -\frac{\text{sign}(j)\Delta_\alpha}{2\pi} \sum_{h\alpha} \int \frac{d\varepsilon_{\alpha hk} \Gamma_{\alpha hj}(\varepsilon_{\alpha hk}) \left(\frac{1}{\omega \mp \varepsilon_{\alpha h-k}} - \frac{1}{\omega \pm \varepsilon_{\alpha-h-k}} \right) \beta_{\alpha \text{sign}(j)hk}^2 \beta_{\alpha \text{sign}(-j)hk}^2}{\omega \mp \varepsilon_{\alpha hk} - \frac{\Delta_\alpha^2}{4} \xi_{\alpha hk \pm j} \left(\frac{\beta_{\alpha \text{sign}(\pm j)hk}^2}{\omega \pm \varepsilon_{\alpha h-k}} + \frac{\beta_{\alpha \text{sign}(\mp j)hk}^2}{\omega \pm \varepsilon_{\alpha-h-k}} \right)}, \quad (\text{A16})$$

with the notation $\xi_{\alpha hk j} = \beta_{\alpha \text{sign}(-j)hk}^2 + \beta_{\alpha \text{sign}(j)hk} \beta_{\alpha \text{sign}(-j)hk}$. The coupling strength $\Gamma_{\alpha hj}(\varepsilon_{\alpha hk}) = \Gamma_{0\alpha} \rho_{\alpha hj}(\varepsilon_{\alpha hk})$ with $\Gamma_{0\alpha} = \pi |\tilde{V}_\alpha|^2 / 2D_\alpha$, where D_α is the half-band width of the leads. The density of states $\rho_{\alpha hj}(\varepsilon_{\alpha hk}) = \frac{k}{\pi d\varepsilon_{\alpha hk}/dk} \beta_{\alpha \text{sign}(j)hk}^2$ can be explicitly written as

$$\rho_{\alpha hj}(\varepsilon_{\alpha hk}) = \begin{cases} \frac{m}{8\pi\hbar^2} \frac{\varepsilon_{\alpha R} - \text{sign}(j)V_{\alpha z}}{2\sqrt{\varepsilon_{\alpha R}(\varepsilon_{\alpha hk} - \tilde{\varepsilon}_{\alpha 0})}} \Theta(2\varepsilon_{\alpha R} - V_{\alpha z}) \delta_{h,-1}; & \tilde{\varepsilon}_{\alpha 0} < \varepsilon_{\alpha hk} < E_{\alpha 0} - V_{\alpha z}, \\ \frac{m}{8\pi\hbar^2} \left(\frac{1}{2} - h \frac{\varepsilon_{\alpha R} - \text{sign}(j)V_{\alpha z}}{2\sqrt{\varepsilon_{\alpha R}(\varepsilon_{\alpha hk} - \tilde{\varepsilon}_{\alpha 0})}} \right); & E_{\alpha 0} + hV_{\alpha z} < \varepsilon_{\alpha hk} < D_{\alpha h}, \\ 0 & \text{otherwise,} \end{cases} \quad (\text{A17})$$

where $D_{\alpha h} = D_\alpha + 2h\sqrt{(D_\alpha - E_{0\alpha} + \frac{V_{\alpha z}^2}{4\varepsilon_{\alpha R}})\varepsilon_{\alpha R}}$, $E_{\alpha 0}$ is the bottom of the conduction band without spin-orbit coupling, $\varepsilon_{\alpha R} = m\lambda_\alpha^2/2$ is the energy of the RSOC, and the notation $\tilde{\varepsilon}_{\alpha 0} = E_{\alpha 0} - \varepsilon_{\alpha R} - V_{\alpha z}^2/4\varepsilon_{\alpha R}$.

Furthermore, we rewrite the dot GF [see Eq. (A14)] in a concise form,

$$\hat{G}_j(\omega) = \hat{G}_j^0(\omega) + \hat{\Sigma}_j^U(\omega), \quad (\text{A18})$$

where

$$[\hat{G}_j^0(\omega)]^{-1} = \hat{I}\omega - \sigma_z \text{diag}(\varepsilon_j, \varepsilon_{-j}) - \hat{\Sigma}_j^0(\omega) \quad (\text{A19})$$

is the noninteracting GF, $\hat{\Sigma}_j^0(\omega)$ is the noninteracting self-energy explicitly expressed in Eqs. (A15) and (A16), and $\hat{\Sigma}_j^U(\omega) = U\hat{G}_j^0(\omega)\hat{F}_{dj}(\omega)$ is the interacting self-energy with

$$\hat{F}_{dj}(\omega) = \begin{pmatrix} \langle\langle d_j n_{-j}; d_j^\dagger \rangle\rangle & \langle\langle d_j n_{-j}; d_{-j} \rangle\rangle \\ -\langle\langle d_{-j}^\dagger n_j; d_j^\dagger \rangle\rangle & -\langle\langle d_{-j}^\dagger n_j; d_{-j} \rangle\rangle \end{pmatrix}. \quad (\text{A20})$$

In general, it is difficult to treat the interacting self-energy $\hat{\Sigma}_j^U(\omega)$ exactly by the theoretical and numerical approaches in all parameter regions [46–49]. The off-diagonal element of $\hat{F}_{dj}(\omega)$ stands for the superconducting correlations on the dot level, which can be approximately given by the Hartree-Fock approximation (HFA), such as $\langle\langle d_{-j}^\dagger n_j; d_j^\dagger \rangle\rangle = \langle n_j \rangle \langle\langle d_{-j}^\dagger; d_j^\dagger \rangle\rangle - \langle d_j^\dagger d_{-j}^\dagger \rangle \langle\langle d_j; d_j^\dagger \rangle\rangle$. Then, we obtain

$$\langle\langle d_{-j}^\dagger; d_j^\dagger \rangle\rangle = \frac{\hat{\Sigma}_{j21}^0(\omega) + U\langle d_j^\dagger d_{-j}^\dagger \rangle}{\omega + \varepsilon_{-j} + U\langle n_j \rangle - \hat{\Sigma}_{j11}^0(\omega)} \langle\langle d_j; d_j^\dagger \rangle\rangle. \quad (\text{A21})$$

Here, we should point out that the superconducting correlation at the QD is significantly suppressed by Coulomb repulsion due to $U \gg \Delta_\alpha$. Thus, the HFA in the off-diagonal parts of $\hat{F}_{dj}(\omega)$ is good enough [22,63]. However, it is well known that the HFA cannot capture the Kondo physics, and one needs to consider the high-order GFs in the diagonal parts of $\hat{F}_{dj}(\omega)$. In the present work, we truncate the hierarchy of GFs by the Lacroix scheme [50]. It qualitatively captures the Kondo effect even at zero temperature [60] and particle-hole symmetry [55]. Although the EOM approach tends to underestimate the Kondo temperature, it can properly capture the competition between the Kondo effect and superconductivity [17,22].

In the following, we show the main steps to obtain the diagonal elements of the dot GF in the frame of Lacroix's approximation. From Eq. (A9), the EOM of the high-order GF $[\hat{F}_{dj}(\omega)]_{11}$ is

$$\begin{aligned} & (\omega - \varepsilon_j - U) \langle\langle d_j n_{-j}; d_j^\dagger \rangle\rangle \\ &= \langle n_{-j} \rangle + \sum_{h\alpha} h^{j+1/2} \int dk \beta_{\alpha \text{sign}(-j)hk} \tilde{V}_\alpha [\langle\langle d_{-j}^\dagger c_{\alpha hk-j} d_j; d_j^\dagger \rangle\rangle - \langle\langle c_{\alpha hk-j}^\dagger d_{-j} d_j; d_j^\dagger \rangle\rangle + \langle\langle c_{\alpha hk} n_{-j}; d_j^\dagger \rangle\rangle]. \end{aligned} \quad (\text{A22})$$

The EOM of the high-order GFs involved in Eq. (A22) can be read as

$$\begin{aligned} & (\omega - \varepsilon_{\alpha hk}) \langle\langle c_{\alpha hk} n_{-j}; d_j^\dagger \rangle\rangle \\ &= \Delta_\alpha \sum_{h'} \beta_{\alpha-hk} \beta_{\alpha h'-k} [\delta_{j,1/2} h \langle\langle c_{\alpha h'-k}^\dagger n_{-j}; d_j^\dagger \rangle\rangle - \delta_{j,-1/2} h' \langle\langle c_{\alpha h'-k}^\dagger n_{-j}; d_j^\dagger \rangle\rangle] + h^{-j+1/2} \tilde{V}_\alpha \beta_{\alpha \text{sign}(j)hk} \langle\langle d_j n_{-j}; d_j^\dagger \rangle\rangle \\ &+ \sum_{h'\alpha'} h'^{j+1/2} \int dk' \tilde{V}_{\alpha'} \beta_{\alpha' \text{sign}(-j)h'k'} [\langle\langle c_{\alpha hk} d_{-j}^\dagger c_{\alpha' h'k'}; d_j^\dagger \rangle\rangle - \langle\langle c_{\alpha' h'k'}^\dagger d_{-j} c_{\alpha hk}; d_j^\dagger \rangle\rangle], \end{aligned} \quad (\text{A23})$$

$$\begin{aligned}
& (\omega - \varepsilon_{\alpha hk} + \varepsilon_{-j} - \varepsilon_j) \langle \langle d_{-j}^\dagger c_{\alpha hk-j} d_j; d_j^\dagger \rangle \rangle \\
&= \sum_{h'\alpha'} \int dk \tilde{V}_{\alpha'} [h'^{-j+1/2} \beta_{\alpha' \text{sign}(j)h'k'} \langle \langle d_{-j}^\dagger c_{\alpha hk-j} c_{\alpha' h'k' j}; d_j^\dagger \rangle \rangle - h'^{j+1/2} \beta_{\alpha' \text{sign}(-j)h'k'} \langle \langle c_{\alpha' h'k' -j}^\dagger c_{\alpha hk-j} d_j; d_j^\dagger \rangle \rangle] \\
&+ \langle d_{-j}^\dagger c_{\alpha hk-j} \rangle + \Delta_\alpha \sum_{h'} \beta_{\alpha-hk} \beta_{\alpha h'-k} [\delta_{-j,1/2} h \langle \langle d_{-j}^\dagger c_{\alpha h' -kj}^\dagger d_j; d_j^\dagger \rangle \rangle - \delta_{j,1/2} h' \langle \langle d_{-j}^\dagger c_{\alpha h' -kj}^\dagger d_j; d_j^\dagger \rangle \rangle] \\
&+ h^{j+1/2} \tilde{V}_\alpha \beta_{\alpha \text{sign}(-j)hk} \langle \langle n_{-j} d_j; d_j^\dagger \rangle \rangle, \tag{A24}
\end{aligned}$$

and

$$\begin{aligned}
& (\omega + \varepsilon_{\alpha hk} - \varepsilon_{-j} - \varepsilon_j - U) \langle \langle c_{\alpha hk-j}^\dagger d_{-j} d_j; d_j^\dagger \rangle \rangle \\
&= \sum_{h'\alpha'} \int dk \tilde{V}_{\alpha'} [h'^{-j+1/2} \beta_{\alpha' \text{sign}(j)h'k'} \langle \langle c_{\alpha hk-j}^\dagger d_{-j} c_{\alpha' h'k' j}; d_j^\dagger \rangle \rangle + h'^{j+1/2} \beta_{\alpha' \text{sign}(-j)h'k'} \langle \langle c_{\alpha hk-j}^\dagger c_{\alpha' h'k' -j} d_j; d_j^\dagger \rangle \rangle] \\
&+ \langle c_{\alpha hk-j}^\dagger d_{-j} \rangle + \Delta_\alpha \sum_h \beta_{\alpha-hk} \beta_{\alpha h'-k} [\delta_{j,1/2} h \langle \langle c_{\alpha hk-j} d_{-j} d_j; d_j^\dagger \rangle \rangle - \delta_{j,-1/2} h' \langle \langle c_{\alpha hk-j} d_{-j} d_j; d_j^\dagger \rangle \rangle] \\
&- \tilde{V}_\alpha h^{j+1/2} \beta_{\alpha \text{sign}(-j)hk} \langle \langle n_{-j} d_j; d_j^\dagger \rangle \rangle. \tag{A25}
\end{aligned}$$

Based on these equations, the Lacroix treatment can be reached by taking the approximation, e.g., $\langle \langle c_{\alpha hk} d_{-j}^\dagger c_{\alpha' h'k' -j}; d_j^\dagger \rangle \rangle \approx \langle d_{-j}^\dagger c_{\alpha' h'k' -j} \rangle \langle \langle c_{\alpha hk}; d_j^\dagger \rangle \rangle + \langle c_{\alpha' h'k' -j} c_{\alpha hk} \rangle \langle \langle d_{-j}^\dagger; d_j^\dagger \rangle \rangle$, $\langle \langle c_{\alpha' h'k' -j}^\dagger d_{-j} c_{\alpha hk} j; d_j^\dagger \rangle \rangle \approx \langle c_{\alpha' h'k' -j}^\dagger d_{-j} \rangle \langle \langle c_{\alpha hk} j; d_j^\dagger \rangle \rangle + \langle d_{-j} c_{\alpha hk} j \rangle \langle \langle c_{\alpha' h'k' -j}^\dagger; d_j^\dagger \rangle \rangle$, and $\langle \langle d_{-j}^\dagger c_{\alpha hk-j} c_{\alpha' h'k' j}; d_j^\dagger \rangle \rangle \approx \langle d_{-j}^\dagger c_{\alpha hk-j} \rangle \langle \langle c_{\alpha' h'k' j}; d_j^\dagger \rangle \rangle + \langle c_{\alpha hk-j} c_{\alpha' h'k' j} \rangle \langle \langle d_{-j}^\dagger; d_j^\dagger \rangle \rangle$. Furthermore, we can neglect the terms containing the superconducting correlation on the dot due to $U \gg \Delta$, such as $\langle \langle c_{\alpha h' -k-j}^\dagger n_{-j}; d_j^\dagger \rangle \rangle$, $\langle \langle d_{-j}^\dagger c_{\alpha h' -kj}^\dagger d_j; d_j^\dagger \rangle \rangle$, and $\langle \langle c_{\alpha h' -k-j} d_{-j} d_j; d_j^\dagger \rangle \rangle$. After some straightforward simplifications, we obtain the high-order GF,

$$\begin{aligned}
\langle \langle d_j n_{-j}; d_j^\dagger \rangle \rangle &= \frac{\langle n_{-j} \rangle + A_{j1}(\omega) - A_{j2}(\omega)}{\omega - \varepsilon_j - U - \Xi_{jT}(\omega)} + \frac{(A_{j1}(\omega) - A_{j2}(\omega)) \hat{\Sigma}_{j21}^0(\omega)}{\omega - \varepsilon_j - U - \Xi_{jT}(\omega)} \langle \langle d_{-j}^\dagger; d_j^\dagger \rangle \rangle + \frac{[A_{j1}(\omega) - A_{j2}(\omega)] \hat{\Sigma}_{j11}^0(\omega)}{\omega - \varepsilon_j - U - \Xi_{jT}(\omega)} \langle \langle d_j; d_j^\dagger \rangle \rangle \\
&- \frac{B_{j1}(\omega) + B_{j2}(\omega)}{\omega - \varepsilon_j - U - \Xi_{jT}(\omega)} \langle \langle d_j; d_j^\dagger \rangle \rangle, \tag{A26}
\end{aligned}$$

where the notation $\Xi_{jT}(\omega) = \Xi_{j0}(\omega) + \Xi_{j1}(\omega) + \Xi_{j2}(\omega)$ with $\Xi_{j0}(\omega) = \sum_{h\alpha} \int dk \frac{\tilde{V}_\alpha^2 \beta_{\alpha \text{sign}(j)hk}^2}{\omega - \varepsilon_{\alpha hk}}$, $\Xi_{j\eta}(\omega) = \sum_{h\alpha} \int dk \frac{\tilde{V}_\alpha^2 \beta_{\alpha \text{sign}(-j)hk}^2}{\omega - \varepsilon_{\eta\alpha hk}}$ ($\eta = 1, 2$), $\varepsilon_{1\alpha hk} = \varepsilon_{\alpha hk} - \varepsilon_{-j} + \varepsilon_j$, and $\varepsilon_{2\alpha hk} = -\varepsilon_{\alpha hk} + \varepsilon_{-j} + \varepsilon_j + U$. Other notations are

$$A_{j\eta}(\omega) = \sum_{h\alpha} h^{j+1/2} \int dk \beta_{\alpha \text{sign}(-j)hk} \frac{\tilde{V}_\alpha \langle d_{-j}^\dagger \tilde{c}_{\alpha hk-j} \rangle}{\omega - \varepsilon_{\eta\alpha hk}} \tag{A27}$$

and

$$B_{j\eta}(\omega) = \sum_{h\alpha} \sum_{h'\alpha'} h'^{j+1/2} h^{j+1/2} \iint dk' dk \beta_{\alpha \text{sign}(-j)hk} \beta_{\alpha' \text{sign}(-j)h'k'} \frac{\tilde{V}_\alpha \tilde{V}_{\alpha'} \langle c_{\alpha' h'k' -j}^\dagger c_{\alpha hk-j} \rangle}{\omega - \varepsilon_{\eta\alpha hk}}. \tag{A28}$$

By substituting Eq. (A26) into Eq. (A14), we obtain the dot GF,

$$\langle \langle d_j; d_j^\dagger \rangle \rangle = \frac{1 + U O_j(\omega) + (1 + U P_j(\omega)) \hat{\Sigma}_{j21}^0(\omega) \hat{G}_j(\omega)_{21}}{\omega - \varepsilon_j - \hat{\Sigma}_{j11}^0(\omega) - U [P_j(\omega) - Q_j(\omega)]}, \tag{A29}$$

where the notations are $O_j(\omega) = \frac{\langle n_{-j} \rangle + A_{j1}(\omega) - A_{j2}(\omega)}{\omega - \varepsilon_j - U - \Xi_{jT}(\omega)}$, $P_j(\omega) = \frac{(A_{j1}(\omega) - A_{j2}(\omega)) \hat{\Sigma}_{j11}^0(\omega)}{\omega - \varepsilon_j - U - \Xi_{jT}(\omega)}$, and $Q_j(\omega) = \frac{B_{j1}(\omega) + B_{j2}(\omega)}{\omega - \varepsilon_j - U - \Xi_{jT}(\omega)}$. In $A_{j\eta}(\omega)$ and $B_{j\eta}(\omega)$, the average values $\langle d_{-j}^\dagger \tilde{c}_{\alpha hk-j} \rangle$ and $\langle \tilde{c}_{\alpha' h'k' -j}^\dagger \tilde{c}_{\alpha hk-j} \rangle$ are given by the spectral theorem,

$$\langle d_{-j}^\dagger \tilde{c}_{\alpha hk-j} \rangle = -\frac{1}{\pi} \text{Im} \int f(\omega) \langle \langle \tilde{c}_{\alpha hk-j}; d_{-j}^\dagger \rangle \rangle d\omega \tag{A30}$$

and

$$\langle \tilde{c}_{\alpha' h'k' -j}^\dagger \tilde{c}_{\alpha hk-j} \rangle = -\frac{1}{\pi} \text{Im} \int f(\omega) \langle \langle \tilde{c}_{\alpha hk-j}; \tilde{c}_{\alpha' h'k' -j}^\dagger \rangle \rangle d\omega. \tag{A31}$$

Based on Eq (A12), we can obtain the GFs,

$$\langle \langle \tilde{c}_{\alpha hk-j}; d_{-j}^\dagger \rangle \rangle \approx h^{j+1/2} \tilde{V}_\alpha \beta_{\alpha \text{sign}(-j)hk}^{-1} \langle \langle d_{-j}; d_{-j}^\dagger \rangle \rangle \Pi_{\alpha h-j11}(\omega, \varepsilon_{\alpha hk}) \tag{A32}$$

and

$$\langle\langle \tilde{c}_{\alpha hk-j}; \tilde{c}_{\alpha' h' k'-j}^\dagger \rangle\rangle \approx \beta_{\alpha \text{sign}(-j)hk}^{-2} \Pi_{\alpha h-j11}(\omega, \varepsilon_{\alpha hk}), \quad (\text{A33})$$

where the notation $\Pi_{\alpha h-j11}(\omega, \varepsilon_{\alpha hk}) = \beta_{\alpha \text{sign}(-j)hk}^2 [\omega - \varepsilon_{\alpha hk} - \frac{\Delta_{\alpha}^2}{4} \xi_{\alpha hk-j} (\frac{\beta_{\alpha \text{sign}(-j)hk}^2}{\omega + \varepsilon_{\alpha h-k}} + \frac{\beta_{\alpha \text{sign}(j)hk}^2}{\omega + \varepsilon_{\alpha h-k}})]^{-1}$. Taking some simplification procedures, we gain

$$A_{j\eta}(\omega) = \frac{i}{\pi^2} \sum_{h\alpha} \int d\varepsilon_{\alpha hk} \frac{\Gamma_{\alpha hj}(\varepsilon_{\alpha hk}) \Theta_{\alpha hj}(\varepsilon_{\alpha hk})}{\omega - \varepsilon_{\eta \alpha hk j}} \quad (\text{A34})$$

and

$$B_{j\eta}(\omega) = \frac{i}{\pi^2} \sum_{h\alpha} \int d\varepsilon_{\alpha hk} \frac{\Gamma_{\alpha hj}(\varepsilon_{\alpha hk}) \Lambda_{\alpha hj}(\varepsilon_{\alpha hk})}{\omega - \varepsilon_{\eta \alpha hk j}}, \quad (\text{A35})$$

where $\Theta_{\alpha hj}(\varepsilon_{\alpha hk}) = \int f(\omega)(\omega + \varepsilon_{\alpha hk}) \Pi_{\alpha h-j11}(\omega, \varepsilon_{\alpha hk}) \hat{G}_{-j}(\omega)_{11} d\omega$ and $\Lambda_{\alpha hj}(\varepsilon_{\alpha hk}) = \int f(\omega)(\omega + \varepsilon_{\alpha hk}) \Pi_{\alpha h-j11}(\omega, \varepsilon_{\alpha hk}) d\omega$.

-
- [1] J. Kondo, *Prog. Theor. Phys.* **32**, 37 (1964).
[2] K. G. Wilson, *Rev. Mod. Phys.* **47**, 773 (1975).
[3] A. C. Hewson, *The Kondo Problem to Heavy Fermions* (Cambridge University Press, Cambridge, 1993).
[4] D. Goldhaber-Gordon, H. Shtrikman, D. Mahalu, D. Abusch-Magder, U. Meirav, and M. A. Kastner, *Nature (London)* **391**, 156 (1998).
[5] S. M. Cronenwett, T. H. Oosterkamp, and L. P. Kouwenhoven, *Science* **281**, 540 (1998).
[6] M. R. Buitelaar, T. Nussbaumer, and C. Schönenberger, *Phys. Rev. Lett.* **89**, 256801 (2002).
[7] C. Buizert, A. Oiwa, K. Shibata, K. Hirakawa, and S. Tarucha, *Phys. Rev. Lett.* **99**, 136806 (2007).
[8] L. Yu, *Acta Phys. Sin.* **21**, 75 (1965) (in Chinese).
[9] H. Shiba, *Prog. Theor. Phys.* **40**, 435 (1968).
[10] A. I. Rusinov, *Zh. Eksp. Teor. Fiz.* **56**, 2047 (1969) [*Sov. Phys. JETP* **29**, 1101 (1969)].
[11] M. E. Flatté and J. M. Byers, *Phys. Rev. Lett.* **78**, 3761 (1997).
[12] A. A. Clerk and V. Ambegaokar, *Phys. Rev. B* **61**, 9109 (2000).
[13] A. V. Rozhkov and D. P. Arovas, *Phys. Rev. B* **62**, 6687 (2000).
[14] M.-S. Choi, M. Lee, K. Kang, and W. Belzig, *Phys. Rev. B* **70**, 020502(R) (2004).
[15] F. Siano and R. Egger, *Phys. Rev. Lett.* **93**, 047002 (2004); **94**, 039902(E) (2005).
[16] C. Karrasch, A. Oguri, and V. Meden, *Phys. Rev. B* **77**, 024517 (2008).
[17] L. Li, B.-B. Zheng, W.-Q. Chen, H. Chen, H.-G. Luo, and F.-C. Zhang, *Phys. Rev. B* **89**, 245135 (2014).
[18] K. J. Franke, G. Schulze, and J. I. Pascual, *Science* **332**, 940 (2011).
[19] W. Chang, V. E. Manucharyan, T. S. Jespersen, J. Nygard, and C. M. Marcus, *Phys. Rev. Lett.* **110**, 217005 (2013).
[20] B.-K. Kim, Y.-H. Ahn, J.-J. Kim, M.-S. Choi, M.-H. Bae, K. Kang, J. S. Lim, R. López, and N. Kim, *Phys. Rev. Lett.* **110**, 076803 (2013).
[21] J. O. Island, R. Gaudenzi, J. de Bruijckere, E. Burzuri, C. Franco, M. Mas-Torrent, C. Rovira, J. Veciana, T. M. Klapwijk, R. Aguado, and H. S. J. van der Zant, *Phys. Rev. Lett.* **118**, 117001 (2017).
[22] L. Li, M. X. Gao, Z. H. Wang, H. G. Luo, and W. Q. Chen, *Phys. Rev. B* **97**, 064519 (2018).
[23] C. L. Seaman, M. B. Maple, B. W. Lee, S. Ghamaty, M. S. Torikachvili, J.-S. Kang, L. Z. Liu, J. W. Allen, and D. L. Cox, *Phys. Rev. Lett.* **67**, 2882 (1991).
[24] M. Matsumoto and M. Koga, *Phys. Rev. B* **65**, 024508 (2001).
[25] M. Koga and M. Matsumoto, *Phys. Rev. B* **65**, 094434 (2002).
[26] A. V. Balatsky, I. Vekhter, and J.-X. Zhu, *Rev. Mod. Phys.* **78**, 373 (2006).
[27] M. Koga and M. Matsumoto, *J. Nucl. Sci. Technol.* **39**(3), 202 (2002).
[28] L. Fritz and M. Vojta, *Phys. Rev. B* **72**, 212510 (2005).
[29] R. Wang, W. Su, J.-X. Zhu, C. S. Ting, H. Li, C.-F. Chen, B.-G. Wang, and X.-Q. Wang, *Phys. Rev. Lett.* **122**, 087001 (2019).
[30] I. J. Hamad, F. T. Lisandrini, C. J. Gazza, and A. M. Lobos, *Phys. Rev. B* **100**, 235110 (2019).
[31] L. P. Gor'kov and E. I. Rashba, *Phys. Rev. Lett.* **87**, 037004 (2001).
[32] P. A. Frigeri, D. F. Agterberg, A. Koga, and M. Sigrist, *Phys. Rev. Lett.* **92**, 097001 (2004); **93**, 099903(E) (2004).
[33] A. P. Mackenzie and Y. Maeno, *Rev. Mod. Phys.* **75**, 657 (2003).
[34] A. P. Schnyder, S. Ryu, A. Furusaki, and A. W. W. Ludwig, *Phys. Rev. B* **78**, 195125 (2008).
[35] C. Kallin and J. Berlinsky, *Rep. Prog. Phys.* **79**, 054502 (2016).
[36] J. D. Sau, R. M. Lutchyn, S. Tewari, and S. Das Sarma, *Phys. Rev. Lett.* **104**, 040502 (2010).
[37] R. M. Lutchyn, J. D. Sau, and S. Das Sarma, *Phys. Rev. Lett.* **105**, 077001 (2010).
[38] Y. Kim, J. Zhang, E. Rossi, and R. M. Lutchyn, *Phys. Rev. Lett.* **114**, 236804 (2015).
[39] M. Zarea, S. E. Ulloa, and N. Sandler, *Phys. Rev. Lett.* **108**, 046601 (2012).
[40] L. Isaev, D. F. Agterberg, and I. Vekhter, *Phys. Rev. B* **85**, 081107(R) (2012).
[41] R. Zitko and J. Bonca, *Phys. Rev. B* **84**, 193411 (2011).
[42] A. Wong, S. E. Ulloa, N. Sandler, and K. Ingersent, *Phys. Rev. B* **93**, 075148 (2016).
[43] S. Fujimoto, *Phys. Rev. B* **77**, 220501(R) (2008).
[44] C. Zhang, S. Tewari, R. M. Lutchyn, and S. Das Sarma, *Phys. Rev. Lett.* **101**, 160401 (2008).
[45] J. Alicea, *Phys. Rev. B* **81**, 125318 (2010); *Rep. Prog. Phys.* **75**, 076501 (2012).

- [46] R. Bulla, T. A. Costi, and T. Pruschke, *Rev. Mod. Phys.* **80**, 395 (2008).
- [47] F. M. Hu, T.-X. Ma, H.-Q. Lin, and J. E. Gubernatis, *Phys. Rev. B* **84**, 075414 (2011).
- [48] P. Coleman, *Phys. Rev. B* **29**, 3035 (1984); **35**, 5072 (1987).
- [49] N. E. Bickers, *Rev. Mod. Phys.* **59**, 845 (1987).
- [50] C. Lacroix, *J. Phys. F* **11**, 2389 (1981).
- [51] H.-G. Luo, Z.-J. Ying, and S.-J. Wang, *Phys. Rev. B* **59**, 9710 (1999).
- [52] M. Krawiec and K. I. Wysokiński, *Supercond. Sci. Technol.* **17**, 103 (2004).
- [53] T. Domański, A. Donabidowicz, and K. I. Wysokiński, *Phys. Rev. B* **78**, 144515 (2008).
- [54] Y. Qi, J.-X. Zhu, S. Zhang, and C. S. Ting, *Phys. Rev. B* **78**, 045305 (2008).
- [55] Y. Qi, J. X. Zhu, and C. S. Ting, *Phys. Rev. B* **79**, 205110 (2009).
- [56] T.-F. Fang, W. Zuo, and H.-G. Luo, *Phys. Rev. Lett.* **101**, 246805 (2008); **104**, 169902(E) (2010).
- [57] Q. Feng, Y.-Z. Zhang, and H. O. Jeschke, *Phys. Rev. B* **79**, 235112 (2009).
- [58] J. Barański and T. Domański, *Phys. Rev. B* **84**, 195424 (2011).
- [59] D. Krychowski, J. Kaczkowski, and S. Lipinski, *Phys. Rev. B* **89**, 035424 (2014).
- [60] V. Kashcheyevs, A. Aharony, and O. Entin-Wohlman, *Phys. Rev. B* **73**, 125338 (2006).
- [61] L. Li, Z. Cao, T. F. Fang, H. G. Luo, and W. Q. Chen, *Phys. Rev. B* **94**, 165144 (2016).
- [62] J. C. Cuevas, A. Levy Yeyati, and A. Martín-Rodero, *Phys. Rev. B* **63**, 094515 (2001).
- [63] E. Vecino, A. Martín-Rodero, and A. Levy Yeyati, *Phys. Rev. B* **68**, 035105 (2003).
- [64] A. Golub, I. Kuzmenko, and Y. Avishai, *Phys. Rev. Lett.* **107**, 176802 (2011).
- [65] M. Lee, J.-S. Lim, and R. López, *Phys. Rev. B* **87**, 241402(R) (2013).
- [66] S. Glodzik, A. Kobialka, A. Gorczyca-Goraj, A. Ptok, G. Gorski, M. M. Maska, and T. Domanski, *Beilst. J. Nanotechnol.* **9**, 1370 (2018).
- [67] R. Chirla, I. V. Dinu, V. Moldoveanu, and C. P. Moca, *Phys. Rev. B* **90**, 195108 (2014).
- [68] D. E. Liu, M. Cheng, and R. M. Lutchyn, *Phys. Rev. B* **91**, 081405(R) (2015).
- [69] D. A. Ruiz-Tijerina, E. Vernek, L. G. G. V. Dias da Silva, and J. C. Egues, *Phys. Rev. B* **91**, 115435 (2015).
- [70] I. J. van Beek and B. Braunecker, *Phys. Rev. B* **94**, 115416 (2016).
- [71] I. Weymann and K. P. Wojcik, *Phys. Rev. B* **95**, 155427 (2017).
- [72] M. Cheng, M. Becker, B. Bauer, and R. M. Lutchyn, *Phys. Rev. X* **4**, 031051 (2014).
- [73] J. J. He, T. K. Ng, P. A. Lee, and K. T. Law, *Phys. Rev. Lett.* **112**, 037001 (2014).
- [74] A. Haim, E. Berg, F. von Oppen, and Y. Oreg, *Phys. Rev. Lett.* **114**, 166406 (2015).
- [75] J.-P. Xu, M.-X. Wang, Z. L. Liu, J.-F. Ge, X. Yang, C. Liu, Z. A. Xu, D. Guan, C. L. Gao, D. Qian, Y. Liu, Q.-H. Wang, F.-C. Zhang, Q.-K. Xue, and J.-F. Jia, *Phys. Rev. Lett.* **114**, 017001 (2015).
- [76] T. Kawakami and X. Hu, *Phys. Rev. Lett.* **115**, 177001 (2015).
- [77] D. Sticlet, C. Bena, and P. Simon, *Phys. Rev. Lett.* **108**, 096802 (2012).
- [78] M. Leijnse and K. Flensberg, *Phys. Rev. Lett.* **107**, 210502 (2011).
- [79] R. Shindou, A. Furusaki, and N. Nagaosa, *Phys. Rev. B* **82**, 180505(R) (2010).
- [80] D. N. Zubarev, *Usp. Fiz. Nauk* **71**, 71 (1960) [*Sov. Phys. Usp.* **3**, 320 (1960)].